Proceedings of the ASME 2011 Internal Combustion Engine Division Fall Technical Conference
ICEF2011
October 2-5, 2011, Morgantown, West Virginia, USA

ICEF2011-60080

ANALYSIS OF IGNITION BEHAVIOR IN A TURBOCHARGED DIRECT INJECTION DUAL FUEL ENGINE USING PROPANE AND METHANE AS PRIMARY FUELS

A. C. Polk **C. M. Gibson**

N. T. Shoemaker **K. K. Srinivasan** **S. R. Krishnan**[†]

Department of Mechanical Engineering, Mississippi State University, Mississippi State, MS 39762, USA

[†]Corresponding Author: krishnan@me.msstate.edu

ABSTRACT

This paper presents experimental analyses of the ignition delay (ID) behavior for diesel-ignited propane and diesel-ignited methane dual fuel combustion. Two sets of experiments were performed at a constant speed (1800 rev/min) using a 4-cylinder direct injection diesel engine with the stock ECU and a wastegated turbocharger. First, the effects of fuel-air equivalence ratios (Φ_{pilot} ~ 0.2-0.6 and $\Phi_{overall}$ ~ 0.2-0.9) on IDs were quantified. Second, the effects of gaseous fuel percent energy substitution (PES) and brake mean effective pressure (BMEP) (from 2.5 to 10 bar) on IDs were investigated. With constant Φ_{pilot} (> 0.5), increasing $\Phi_{overall}$ with propane initially decreased ID but eventually led to premature propane autoignition; however, the corresponding effects with methane were relatively minor. Cyclic variations in the start of combustion (SOC) increased with increasing $\Phi_{overall}$ (at constant Φ_{pilot}), more significantly for propane than for methane. With increasing PES at constant BMEP, the ID showed a nonlinear (initially increasing and later decreasing) trend at low BMEPs for propane but a linearly decreasing trend at high BMEPs. For methane, increasing PES only increased IDs at all BMEPs. At low BMEPs, increasing PES led to significantly higher cyclic SOC variations and SOC advancement for both propane and methane. Finally, the engine ignition delay (EID) was also shown to be a useful metric to understand the influence of ID on dual fuel combustion.

NOMENCLATURE

AHRR	Apparent Heat Release Rate
a. u.	Arbitrary Units
BDC	Bottom Dead Center
BMEP	Brake Mean Effective Pressure
EGR	Exhaust Gas Recirculation
EID	Engine Ignition Delay
GETDC	Gas Exchange Top Dead Center
ID	Ignition Delay
IMEP	Indicated Mean Effective Pressure
LHV	Lower Heating Value
MPRR	Maximum Pressure Rise Rate
PES	Percent Energy Substitution
SOC	Start of Combustion
SOI	Start of Injection of Pilot Fuel
TDC	Top Dead Center

1. INTRODUCTION

The increasing need for improved fuel economy and reduced pollutant emissions from internal combustion engines has refocused attention on combustion strategies that achieve highly efficient, clean combustion over a wide range of engine operating conditions. Also, energy security and sustainability concerns have driven the search for suitable alternatives to conventional petroleum fuels such as gasoline and diesel. Faced with these challenges, dual fuel combustion has received renewed interest due to its well-known emissions benefits compared to conventional diesel combustion [1-3]. Dual fuel engines offer the ability to operate on a variety of alternative fuels, while maintaining good fuel conversion efficiencies at high loads and producing low exhaust emissions of oxides of nitrogen (NO_x) and particulate matter (PM). On the other hand, dual fuel combustion can also lead to higher levels of unburned hydrocarbons and carbon monoxide emissions, especially at low loads.

In dual fuel engines, a significant fraction of the fuel chemical energy arises from a low-cetane fuel (usually gaseous) inducted

with the intake air to form a lean premixed fuel-air mixture, which is ignited with timed injection of a high-cetane pilot fuel (e.g., diesel) near top dead center (TDC). Some commonly used gaseous fuels in dual fuel engine applications include methane (the primary component of natural gas), propane, and a variety of other low heating value fuels such as producer gas, landfill gas, and biogas [1]. In the United States, methane and propane are very attractive for stationary power generation and other off-highway applications because of the existing infrastructure for production and delivery of these fuels. Moreover, the conversion of existing diesel engines to operate in dual fuel mode requires very little change to the engine hardware; consequently, these engines retain their ability to operate solely on diesel, if necessary.

A significant amount of research [1-4, 6-8] has been performed to understand the performance and emissions characteristics of dual fuel engines utilizing propane and methane as the primary fuels. Methane is one of the most popular primary fuels used in dual fuel applications due to its excellent resistance to knock (which facilitates high compression ratio operation) and relatively high lower heating value (LHV) compared to diesel [1,9]. Propane is also attractive in terms of its energy content but exhibits relatively weaker knock resistance compared to methane. While the increased reactivity of propane results in faster burn rates and potentially higher brake thermal efficiencies, the engine operating range (viable speeds and loads) may be limited by either end-gas knock or premature propane autoignition.

1.1 The Ignition Delay Period in Dual Fuel Engines

Combustion in a dual fuel engine typically takes place after an ignition delay (ID) period. The ID period in dual fuel engines has been studied for several years [10-14] but requires further investigation to quantify the effects of specific variables (e.g., overall equivalence ratio, percent energy substitution (PES), etc.) on the magnitude of the ID period. Understanding the ID period is important as it influences the ensuing combustion process as well as engine performance and emissions. Ignition delay is defined as the period from the start of injection (SOI) of the pilot fuel to the start of combustion (SOC). The length of ID is primarily governed by the gaseous fuel used, the intake temperature, the pilot injection timing, and the overall equivalence ratio [11]. A typical trend observed by Liu et al. [12] using natural gas as the primary fuel shows that for a given pilot quantity, ID will increase to a peak as the overall equivalence ratio is increased, decrease to a minimum before the stoichiometric ratio, and then increase again toward misfire as the stoichiometric ratio is approached and surpassed. In any case, it is well known that ID in dual fuel engines is affected with increasing PES and increasing equivalence ratio. The primary objective of the present work is characterizing dual fuel ID behavior with both propane and methane as primary fuels.

2. OBJECTIVES

The specific objectives of this work are as follows:

1. Investigate ignition behavior for dual fuel combustion on a stock Volkswagen (VW) 1.9L turbocharged direct injection (TDI) engine with a stock ECU using in-cylinder combustion data.
2. Compare diesel-ignited methane and diesel-ignited propane dual fuel combustion IDs for a range of equivalence ratios and a range of engine loads and PES at a constant engine speed of 1800 rev/min.
3. Quantify ignition delay effects on dual fuel combustion using engine ignition delays (EID) and cyclic variation plots of SOC.

3. EXPERIMENTAL APPROACH

All experiments in the present work were performed using a VW 1.9L TDI, inline 4-cylinder diesel engine. The overall experimental setup was similar to that described in Gibson et al. [16]. Relevant engine and fuel details are provided in Table 1.

Table 1. Engine and Fuel Specifications

Parameter	Value
Engine	VW 1.9L TDI
Bore	95.5 mm
Stroke	87.5 mm
Connecting rod length	144.4 mm
Nominal compression ratio	19.5:1
Displaced volume	1.9L
Injection system	Mechanical w/ ECU control
Aspiration	Turbocharged with wastegated turbo
Nominal pilot injection timing (degrees CA BTDC)	4
No. 2 diesel cetane number (measured)	47.7
Propane purity	99.5%
Methane purity	99.97%
Lower heating value of diesel (kJ/kg)	42,566
Lower heating value of propane (kJ/kg)	46,400
Lower heating value of methane (kJ/kg)	50,000

Since the stock ECU was utilized along with the mechanical injection system and the wastegated turbocharger in the experiments, engine speed, throttle position (diesel fueling rate), intake manifold (boost) pressure, and gaseous fuel flow rate were the controllable engine parameters. The primary (gaseous) fuel was metered by a manually controlled needle valve, and then introduced into the intake air stream before the turbocharger compressor. The engine speed was controlled

with a Froude Hoffman AG80 (Imperial) eddy current dynamometer and the engine torque was measured with a calibrated load cell. The ECU was used to control diesel injection with a throttle position sensor, which was actuated by the dynamometer control software. A schematic of the experimental setup is shown in Figure 1.

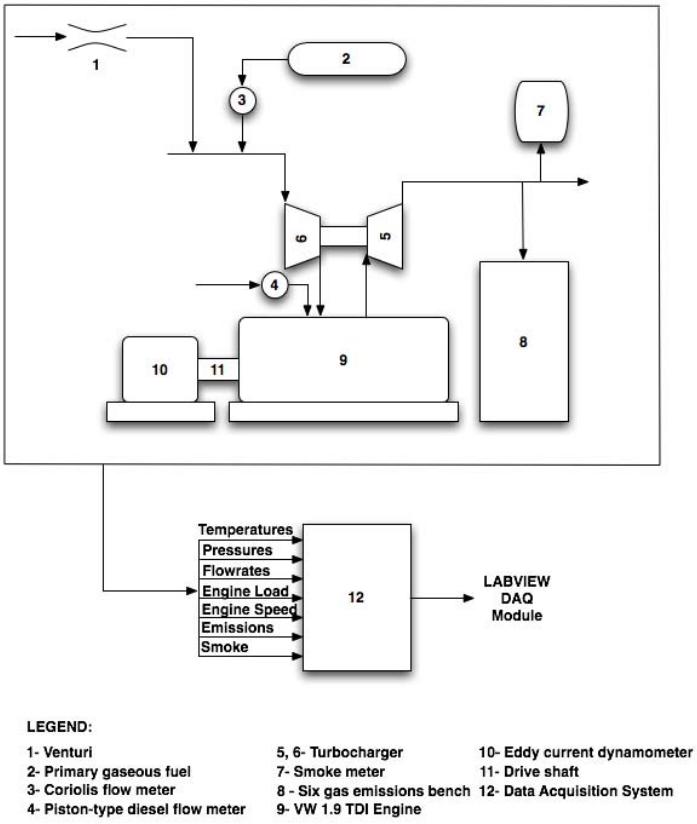

Figure 1. Schematic of the experimental setup.

3.1 Steady State Data Acquisition

Engine coolant temperatures, pre- and post-turbo air temperatures, intake mixture temperature, and post-turbo exhaust temperatures were measured with Omega Type-K thermocouples. A Micro Motion coriolis mass flow meter with 0.35% accuracy (of reading) was used to measure the mass flow of the primary gaseous fuel (methane or propane). Intake air mass flow rates were measured with a FlowMaxx venturi flow meter. Diesel mass flow rate was measured with a Max Machinery Model 213 piston flow meter. Absolute pressure in the test cell was measured with an Omega PX 429 sensor, differential pressure across the venturi air flow meter was measured with a Omega PX429 differential pressure transducer (0.08% best straight line accuracy), and intake boost pressure was measured with a Setra 209 pressure transducer. All gaseous exhaust emissions and smoke were measured downstream of the turbocharger turbine. Gaseous emissions were routed through an emissions sampling trolley to an integrated emissions bench (EGAS 2M) manufactured by *Altech Environnement S.A.* and smoke was measured with an AVL 415S variable sampling smoke meter. All data were collected and post-processed (time-averaged) with a modular LabVIEW based data acquisition system (DAQ) with National Instruments PXI hardware.

3.2 High Speed Data Acquisition

In-cylinder pressure was measured using a Kistler 6065A piezoelectric pressure transducer mounted in a Kistler glow plug adapter. A Kistler 5010B charge amplifier with a medium time constant setting was used to condition the signal output from the piezoelectric pressure transducer. Needle lift was measured using a stock injector that was instrumented with a Wolff needle lift sensor coupled to a signal conditioner. Both in-cylinder pressure and needle lift measurements were recorded with National Instruments PXI S-Series hardware using a BEI shaft encoder of 0.1° crank angle resolution. All in-cylinder data were recorded for 100 successive engine cycles after the engine operation attained steady state. To ensure consistency over all cylinder pressure and heat release measurements, the engine was motored for 40 cycles (and motoring peak pressure locations were verified to occur just before TDC) before firing data were taken to ensure that no slippage of the encoder had occurred.

3.3 Experimental Procedure

All experiments were performed at a constant engine speed of 1800 rev/min without any exhaust gas recirculation (EGR). As shown in Tables 2 and 3, two sets of experiments were performed for both diesel-ignited methane and diesel-ignited propane dual fuel combustion. The first set of experiments focused on understanding the effects of the overall equivalence ratio ($\Phi_{overall}$) on ignition delay behavior for various constant pilot quantity-based equivalence ratios (Φ_{pilot}). For a given pilot quantity (Φ_{pilot}), the amount of primary fuel was increased to increase $\Phi_{overall}$ and the ignition delay behavior was recorded. This process was subsequently repeated for other Φ_{pilot} values. In the second set of experiments, dual fuel ignition delays were examined for increasing PES from the gaseous fuels at different brake mean effective pressures (BMEP). For these tests, the BMEP was monitored and maintained at a specified value while the pilot and primary fuels were adjusted based on predetermined PES increments within ±1.5 percent. The maximum PES stated in Table 3 was dependent on the primary fuel type and the BMEP. If the maximum is not specifically listed for a given condition, then the last stated PES is the maximum for that fuel at that condition.

The relevant engine performance parameters such as pilot equivalence ratio (Φ_{pilot}), overall equivalence ratio ($\Phi_{overall}$), and percent energy substitution (PES) by the primary gaseous fuel are defined below:

$$PES = \frac{\dot{m}_g LHV_g}{\dot{m}_d LHV_d + \dot{m}_g LHV_g} \times 100\% \quad (1)$$

$$\Phi_{pilot} = \frac{\left(A/F\right)_{st-d}}{\left(\frac{\dot{m}_a}{\dot{m}_d}\right)} \quad (2)$$

$$\Phi_{overall} = \frac{\left(A/F\right)_{st-tot}}{\left(\frac{\dot{m}_a}{\dot{m}_d + \dot{m}_g}\right)} \quad (3)$$

In Equations 1 through 3, $\dot{m}$ refers to the mass flow rates of diesel (subscript d), gaseous fuel (subscript g), and air (subscript a), and *LHV* refers to the corresponding lower heating values. Two different stoichiometric air-fuel ratios were defined: (1) $(A/F)_{st\text{-}d}$ based on diesel alone, and (2) $(A/F)_{st\text{-}tot}$, defined as the stoichiometric air required for complete oxidation of both the pilot and the main fuels into CO_2 and H_2O. Therefore, $(A/F)_{st\text{-}tot}$ was dependent on the primary fuel type (methane or propane) as well as the PES with the corresponding primary fuel.

Each set of experiments was performed in the same session to reduce variations in baseline operation and obtain reliable performance and emissions data. In addition, the intake boost pressure was held constant for a given Φ_{pilot} or for a given BMEP. The intake pressure chosen for each condition was based on the nominal boost pressure possible (corresponding to the available exhaust energy) at the baseline condition (no gaseous fuel). Engine coolant temperatures and intake charge temperatures were maintained at 85±5°C and 35±5°C, respectively for all experiments.

Table 2. Experimental Matrix for $\Phi_{overall}$ Effects at Different Φ_{pilot}

Constant Φ_{pilot} →				
Φ_{pilot}	Increase in $\Phi_{overall}$ with gaseous fuel addition			
	+0.1	+0.2	+0.3	+0.4
0.2	M,P	M,P	M	
0.3	M,P	M,P	M	
0.4	M,P	M,P	M,P	
0.5	M,P	M,P	M,P	M
0.6	M,P	M,P		

M: methane dual fueling, P: propane dual fueling

Table 3. Experimental Matrix for PES Effects at Different BMEPs

Constant BMEP →				
BMEP (bar)	Percent Energy Substitution			
	25%	50%	75%	Max
2.5	M,P	M,P	M,P	M,P
5.0	M,P	M		P-47%
7.5	M,P	M,P		
10	M,P	M		P-45%

M: methane dual fueling, P: propane dual fueling

4. DEFINITIONS

4.1 In-cylinder Pressure and Apparent Heat Release Rates

The in-cylinder pressure and apparent heat release rate profiles presented in this work were obtained as the ensemble average of 100 consecutive cycles at a given steady state engine operating condition. After averaging, the data were shifted by an amount determined while motoring the engine (to avoid crossover in the compression and expansion curves in the motoring log P – log V diagram) and scaled by the intake manifold pressure at bottom dead center (BDC) before the compression stroke. In addition to ensemble averaging, the pressure profiles were smoothed by averaging six data points on either side of a given data point to eliminate noise in the pressure data. The apparent heat release was calculated using the following equation [9]:

$$AHRR(\theta) = \frac{\gamma}{\gamma - 1} P \frac{dV}{d\theta} + \frac{1}{\gamma - 1} V \frac{dP}{d\theta} \quad (4)$$

The instantaneous volume (V) was calculated from the known compression ratio, bore, stroke, and connecting rod lengths, and the pressure and volume derivatives ($dP/d\theta$ *and* $dV/d\theta$) were calculated numerically using a fourth order central difference method. The specific heat ratio (γ) was calculated using the correlation given below:

$$\gamma(T) = 4.5333 \times 10^{-8} T^2 - 1.74 \times 10^{-4} T + 1.464667 \quad (5)$$

Global in-cylinder temperature was found using the ideal gas equation of state, and mass trapped was found from the same equation while using the intake manifold temperature, and volume and in-cylinder pressure at intake valve closure (IVC).

4.2 SOI, SOC, and CA50 HR

As the ignition delay period extends from the start of diesel fuel injection (SOI) until the start of combustion (SOC), these

metrics must be defined precisely and consistently. As seen in Fig. 2, in this work, the SOI is defined as the crank angle at which injector needle lift reaches 5 percent of the maximum needle lift for that cycle. Also, the SOC is defined as the crank angle at which the AHRR becomes positive. To eliminate confusion caused as a result of noise in the AHRR curves near SOC (leading to AHRR oscillations about zero and inaccuracies in SOC estimation), the last crank angle at which the AHRR curve becomes positive is taken as the SOC.

Following Kalghatgi et al. [15], the engine ignition delay (EID) is defined as the time elapsed between the SOI and the crank angle at which 50 percent of the cumulative heat release occurs (CA50 HR). As the EID definition incorporates CA50 HR, EID is computed by numerically integrating the AHRR curve from the SOC until the crank angle (determined as CA50 HR) at which the integral becomes one-half of the cumulative heat release. For diesel injection near TDC (as in the present case), the diesel fuel autoignites fairly quickly after injection, before it can mix well with the surrounding air. Kalghatgi et al. [15] defined the EID as a metric to identify the level of diesel-air mixing attained at SOC with straight diesel operation. In general, the higher the EID, the better mixed the diesel is with air at SOC. For dual fuel combustion, the EID can also provide some indication of the rate of combustion of both the pilot diesel fuel and the gaseous fuel. Further, the EID also provides an idea of how combustion phasing is affected by dual fueling.

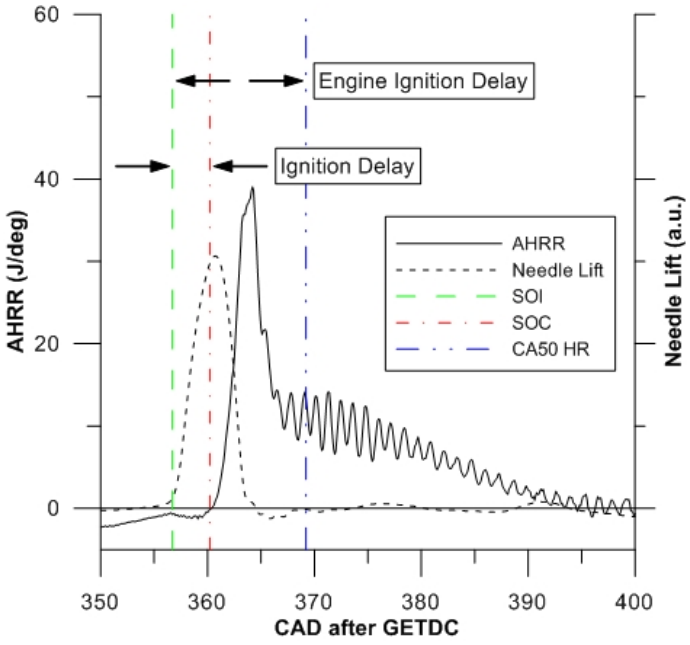

Figure 2. Definitions of SOI, SOC, CA50 HR, ignition delay, and engine ignition delay.

5. RESULTS AND DISCUSSION

The ignition delay period in dual fuel engines is dependent on the primary fuel used, pilot quantity, intake charge temperature, and equivalence ratio [12-14]. In this work the ignition delay behavior of two primary fuels, methane and propane, was investigated over a range of pilot quantities and equivalence ratios while intake temperatures were maintained constant (35±5°C). The experimental matrices shown in Tables 2 and 3 were completed to the extent possible until the onset of engine instability, excessive audible engine noise (*perceived* knock), or a self-imposed maximum pressure rise rate (MPRR) limit of 15 bar/ crank angle degree (CAD) prevented further engine testing. For both propane and methane dual fueling at low BMEPs, the maximum PES of the primary fuel was limited by the onset of misfire or high coefficient of variation of IMEP. At high BMEPs, engine instability limited methane dual fueling whereas extremely high MPRR limited propane dual fueling.

When operating at constant BMEP and varying PES, the pilot quantity was allowed to change with the gaseous fuel substitution, and consequently, the needle lift profile and the maximum needle lift also changed with PES. Therefore, considering the definition used for the SOI (location of 5 percent of the maximum needle lift), if the maximum needle lift changes, the recorded SOI would change even if the actual SOI did not change. A seemingly obvious solution to this problem is to use a constant threshold value for SOI. However, this definition did not work at very high PES (low pilot) where the max needle lift did not even exceed the threshold value. If the threshold was set too low, noise in the needle lift signal yielded a false SOI. Hence, a numerical average was taken of all SOIs based on the definition of 5 percent of the maximum needle lift, which was then used to arrive at a constant nominal SOI of 4 CAD BTDC.

5.1 Ignition in Diesel-Ignited Propane Combustion

5.1.1 Equivalence Ratio Effects on Ignition Delay

The ignition delay trends for diesel-ignited propane combustion are shown for different overall equivalence ratios ($\Phi_{overall}$) in Fig. 3. In this figure, each curve begins with a baseline pilot-based equivalence ratio (Φ_{pilot}) ranging from 0.2 to 0.6 and each data point after the baseline represents an increasingly higher concentration of propane, leading to an overall equivalence ratio ranging from 0.2 to 0.8 or to the extent possible while maintaining stability at lower Φ_{pilot} values. In this test, the pilot quantities are held constant for each Φ_{pilot}. Therefore, "the baseline" at each Φ_{pilot} refers to engine operation with diesel alone (no gaseous fuel addition). At lower Φ_{pilot}, the addition of propane tends to increase the ignition delay slightly. Following Liu and Karim [12], this trend may be attributed to the reduction in in-cylinder

temperature due to the displacement of oxygen in the intake air by the fumigated gaseous fuel (propane) and the increased specific heat ratio of the mixture.

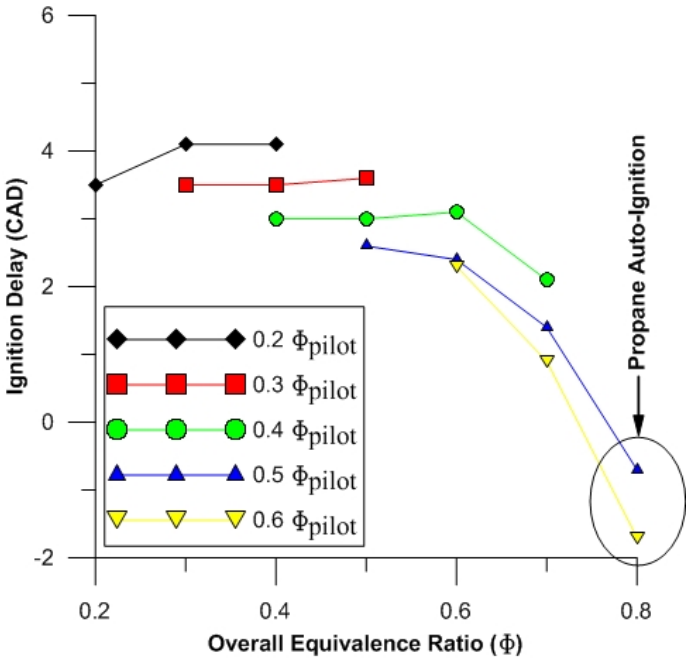

Figure 3. Ignition delay vs. overall equivalence ratio for diesel-ignited propane combustion; BMEPs range from 1 bar to 12.9 bar; boost pressure held constant for each Φ_{pilot} value.

Another possible contributing factor to the ignition delay trends is the pre-ignition chemistry. As the propane-air mixture is compressed in the cylinder, it is exposed to increasingly high temperatures over a relatively long period, allowing ample opportunity for low-temperature preignition reactions. With small diesel pilot quantities, these intermediate products of partial oxidation of propane may compete with diesel ignition, thereby extending the ignition delay period [12]. As Φ_{pilot} (and BMEP) is increased, exhaust temperatures increase dramatically. Thus, as Φ_{pilot} is increased at constant engine speed, the intake fuel-air mixture will be exposed to higher in-cylinder temperatures due to hotter residual exhaust gases and hotter cylinder wall temperatures. Therefore, it is hypothesized that as pilot quantity and BMEP increase, the extent of partial oxidation in the fuel-air mixture increases, further increasing the pressure and temperature in the cylinder. As diesel injection occurs into increasingly high in-cylinder temperatures, diesel evaporation, which is controlled by mixing with the ambient gases, becomes more rapid and the overall ignition delay period is reduced.

As shown in Fig. 3, at relatively high $\Phi_{overall}$ and BMEPs, propane autoignition occurred even before the start of diesel pilot injection. This phenomenon can be observed more closely in Fig. 4. The three cases shown in Fig. 4 employ relatively large pilot quantities (Φ_{pilot} = 0.5 or 0.6) and $\Phi_{overall}$ = 0.7 or 0.8, all at high BMEPs. In the top left plot (Φ_{pilot} = 0.5, $\Phi_{overall}$ = 0.7), the separation between the needle lift (NL) and the negative AHRR due to diesel evaporation after SOI can be seen clearly. Shown below this plot are the cylinder pressure curve and the AHRR curve showing dual fuel combustion progressing normally. The center plots show that with the same Φ_{pilot} and a slight increase in $\Phi_{overall}$ (=0.8), propane begins to autoignite nearly simultaneously with the start of diesel pilot injection, causing very high peak AHRR. The plots in the far-right show that propane clearly autoignites before diesel is injected for Φ_{pilot} = 0.6 and $\Phi_{overall}$ = 0.8, causing more of a staged heat release (with pilot injection not aiding propane heat release until later), which results in a lower peak AHRR. For these conditions where propane autoignites either at or before the SOI, the ambient conditions (high temperatures and high $\Phi_{overall}$) are conducive to preignition reactions in the premixed propane-air mixture to accelerate and release sufficient energy to cause spontaneous ignition. It is important to note that these conditions did not lead to "end-gas knock" that usually follows pilot ignition but premature ignition of propane even before SOI.

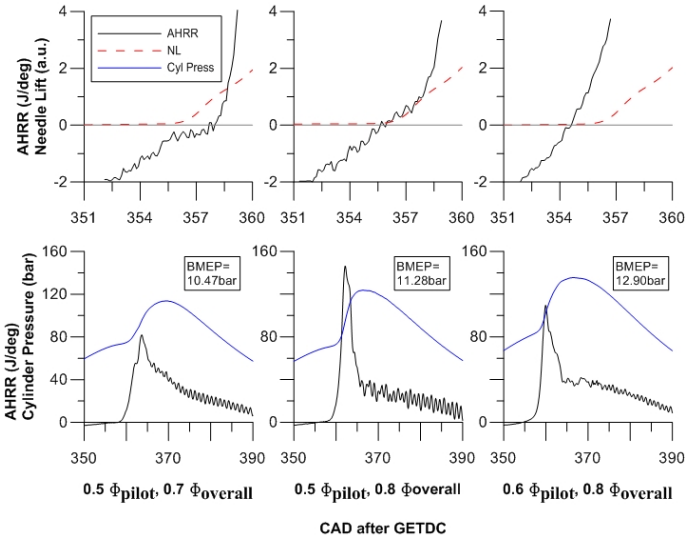

Figure 4. Heat release, needle lift, and cylinder pressure profiles for one normal case (no propane autoignition) and two cases with propane autoignition as shown in Fig. 3.

To examine ignition delay behavior further, Fig. 5 shows the cyclic variations in SOC for a constant Φ_{pilot} of 0.5 and various $\Phi_{overall}$ corresponding to Fig. 3. In this figure, the "baseline" is the condition with Φ_{pilot} = 0.5 and no propane substitution, while each subsequent case refers to increasing propane substitution (e.g., +0.1 phi propane corresponds to $\Phi_{overall}$ = 0.6). At $\Phi_{overall}$ of 0.6 and 0.7, as the propane concentration is increased, the average SOC is advanced (ID is shortened) and the variation in SOC increases. Since intake temperature and intake boost pressure were held constant and no EGR was used, the primary factors influencing ignition behavior were oxygen

displacement, residual exhaust gas temperatures, and propane concentration. As $\Phi_{overall}$ (and BMEP) is increased, the in-cylinder temperatures were likely higher causing the SOC to occur earlier but with greater cyclic variability. However, upon reaching the point of propane autoignition ($\Phi_{overall}$ = 0.8), the variation of SOC begins to decrease significantly.

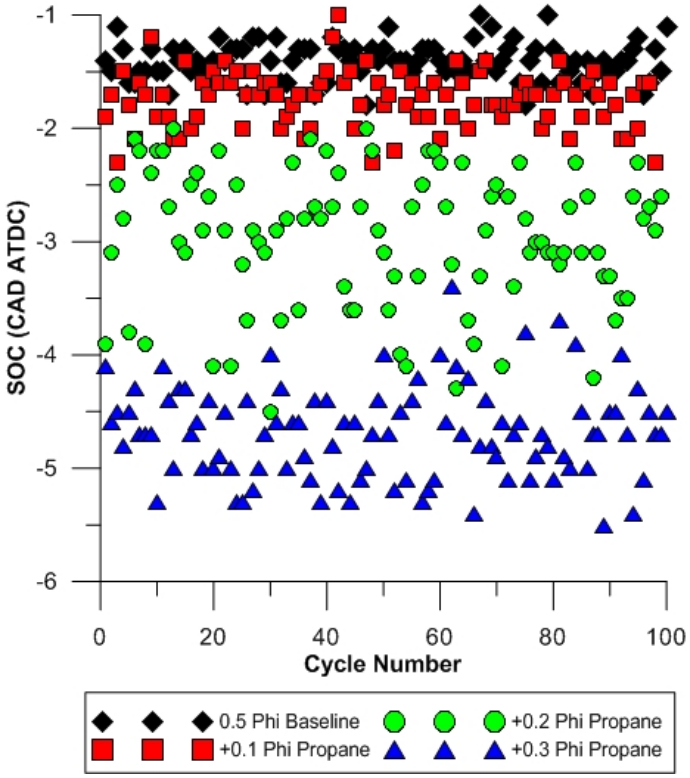

Figure 5. Cyclic variations in SOC for Φ_{pilot} = 0.5 and various propane concentrations ($\Phi_{overall}$ =0.6, 0.7, and 0.8) with a constant boost pressure of 1.4 bar and BMEPs ranging from 7.2 to 11.2 bar; standard deviations of SOC were 0.16, 0.25, 0.6, and 0.4 CAD for $\Phi_{overall}$ = 0.5, 0.6, 0.7, 0.8, respectively.

To clarify the effects of $\Phi_{overall}$ on ignition and the ensuing combustion process, engine ignition delay (EID) trends are shown in Fig. 6. For dual fuel combustion, the EID is a measure of the relative phasing of the combustion process (CA50 HR) with respect to the SOI. The EID increases with increasing Φ_{pilot}. For pure diesel operation at different BMEPs (the first data point in various curves), the EID seems to exhibit a linear trend with increasing BMEP. While increasing Φ_{pilot} decreases ID (see Fig. 3), it also increases the duration of combustion, thus delaying CA50 HR and increasing the overall EID. For a given Φ_{pilot}, increasing propane concentration enriches the homogeneous fuel-air mixture entering the engine. Due to the fact that a greater fraction of the combustion energy is released more rapidly due to flame propagation at higher propane concentrations, EID is decreased. At lower Φ_{pilot}, the increase in EID is attributed to the initial increase in ignition delays with increasing propane concentrations. By contrast, as Φ_{pilot} is increased, the increased reactivity of propane is more pronounced, leading to a significant decrease in EID even with small increases in propane concentration.

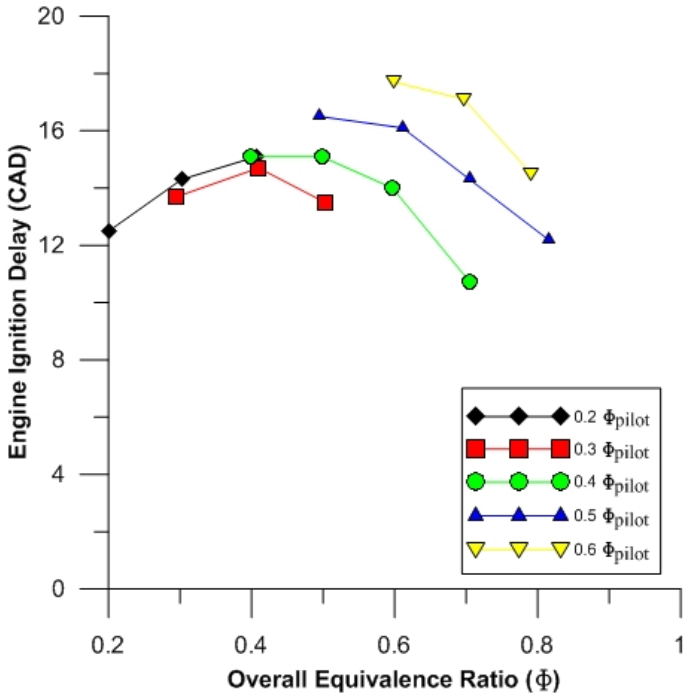

Figure 6. Engine ignition delay vs. overall equivalence ratio for diesel-ignited propane combustion; BMEPs ~ 1 bar to 12.9 bar; boost pressure maintained at baseline Φ_{pilot} value.

5.1.2 Percent Energy Substitution Effects on Ignition Delay

In Fig. 7, the ignition delay behavior of diesel-ignited propane combustion with increasing PES is shown for four constant BMEPs from 2.5 to 10 bar. These results are fundamentally different from the equivalence ratio effects discussed above because the BMEP is held constant while the pilot quantity (Φ_{pilot}) is allowed to vary as PES is increased. At low BMEPs, propane addition initially increases the ignition delay period. However, as the propane concentration reaches a certain point (e.g., 50% PES at 2.5 bar BMEP), the ignition delay begins to decrease. It should be noted here that the maximum PES possible at 2.5 bar BMEP was about 75 percent while for higher BMEPs, the PES was restricted to about 50 percent due to high MPRR values. At higher BMEPs, while the magnitude of ignition delay variation is small, the ignition delay either increases (5 bar BMEP), or remains constant (7.5 bar BMEP), or decreases (10 bar BMEP) as PES is increased. For all of these experiments, the boost pressure was maintained at the baseline diesel value (corresponding to 0% PES), which was a constant for a given BMEP. Since the engine speed was held constant as well, higher BMEPs led to higher exhaust

temperatures and higher boost pressures. The higher exhaust temperatures likely were a consequence of higher in-cylinder mixture temperatures that led to shorter ignition delays. Further, the higher boost pressures at higher BMEPs could have reduced the counteracting effects of oxygen displacement and specific heat ratio modifications with increasing PES. The overall result was a net decrease in ignition delays at higher BMEPs.

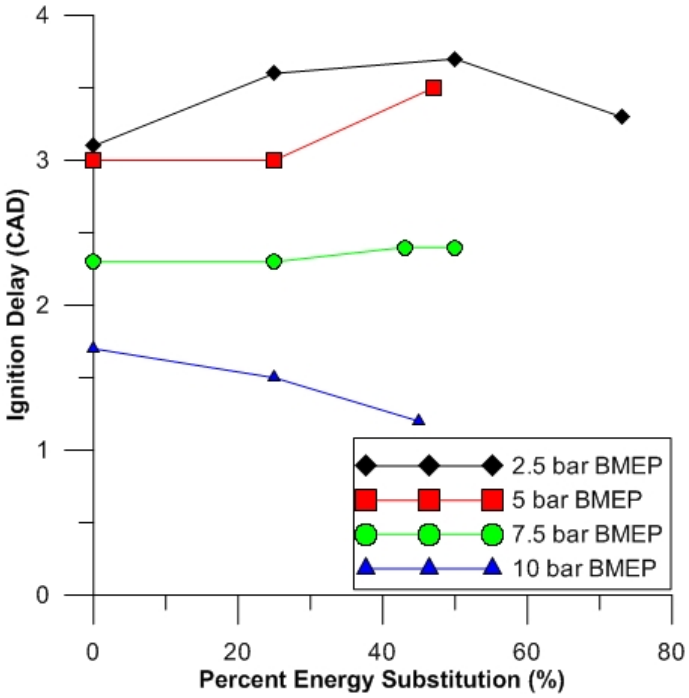

Figure 7. Ignition delay vs. PES at BMEPs of 2.5, 5, 7.5, and 10 bar for diesel-ignited propane combustion. Boost pressure was maintained at 0% PES value for a given BMEP (1.18bar, 1.28 bar, 1.40 bar, and 1.55 bar, respectively).

Figure 8 shows the cyclic variations in SOC for different PES at the 2.5 bar BMEP condition shown in Fig. 7. In contrast to the trends observed in Fig. 5, the differences in SOC behavior with increasing PES are relatively less pronounced. As PES is increased from 0 percent to 25 percent, there is a slight retard in SOC and slightly higher cyclic variations. However, as PES is increased to 50 percent, the cyclic variations in SOC increase substantially. Finally, at 75 percent PES, the average SOC is advanced but the cyclic variations become more significant as the engine operation becomes more unstable (COV of IMEP = 2.9). At 75 percent PES, some cycles experienced more advanced SOC, indicating more pronounced preignition chemical reactions for those cycles. Since the boost pressure was held constant at the baseline value (1.2 bar) corresponding to 0 percent PES, increasing PES increased $\Phi_{overall}$, thus increasing the possibility of preignition reactions in the mixture at higher PES.

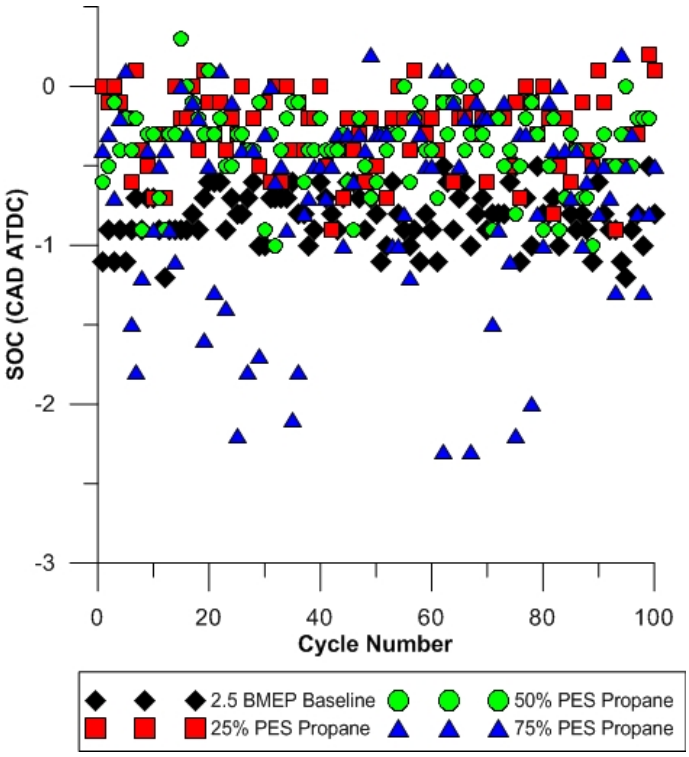

Figure 8. Cyclic variations in SOC for 2.5 bar BMEP and various PES of propane with constant boost pressure of 1.2 bar; standard deviations of SOC were 0.17, 0.24, 0.26, and 0.6 CAD for 0, 25, 50, and 73 percent PES, respectively.

5.2 Ignition in Diesel-Ignited Methane Combustion

5.2.1 Equivalence Ratio Effects on Ignition Delay

Compared to propane, methane is a more stable (less reactive) primary fuel. Therefore, preignition reactions with methane may be relatively weak compared to propane and only the effects of specific heat ratio and oxygen displacement on ignition delay may be significant. As shown in Fig. 9, for a given Φ_{pilot}, the ignition delay remains nearly invariant as $\Phi_{overall}$ is increased. At low BMEPs, increasing $\Phi_{overall}$ leads to a slight increase in ignition delay but at high BMEPs, the changes in ignition delay are relatively small. With constant intake temperatures and methane as the primary fuel, significant ignition delay trends are suppressed with increasing $\Phi_{overall}$, confirming trends reported elsewhere [11,12]. However, with increasing Φ_{pilot}, the ignition delay tends to decrease significantly. This is due to the fact that BMEP increases as Φ_{pilot} is increased and residual exhaust gas temperatures and in-cylinder temperatures are higher, thus leading to shorter ignition delays.

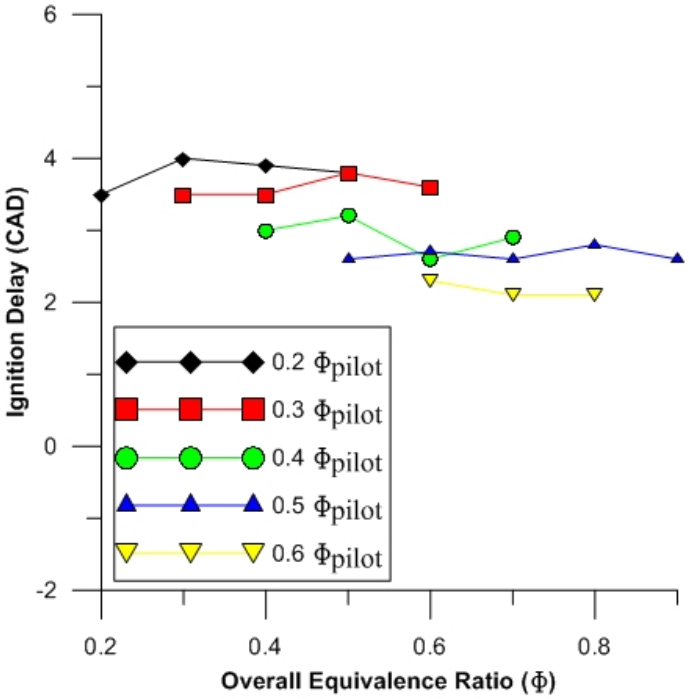

Figure 9. Ignition delay vs. overall equivalence ratio for diesel-ignited methane combustion; BMEPs range from 1 bar to 12.9 bar; boost pressure held constant for each Φ_{pilot} value.

Figure 10 shows the cyclic variations in SOC for diesel-ignited methane combustion at different $\Phi_{overall}$ with the same legend meanings as in Fig. 5. However, these trends are significantly different from the diesel-ignited propane combustion trends shown in Fig. 5. For a constant Φ_{pilot} of 0.5, the SOC remains relatively invariant with increasing methane concentration. This indicates that the injected diesel fuel is the primary contributing factor affecting SOC with very little influence of methane, possibly due to its reduced reactivity compared to propane.

Again, to understand the effects of overall equivalence ratio on combustion phasing in diesel-ignited methane combustion, engine ignition delay trends are shown in Fig. 11. With methane as the primary fuel, the EID trend varies with increasing methane concentration in a manner that is nearly independent of pilot quantity. The EID increases initially with increasing methane concentration, reaches a maximum, and then begins to decrease as methane concentration is further increased. These trends imply that once ignition is achieved with diesel-ignited methane combustion, the phasing of apparent heat release is largely unaffected by the amount of pilot fuel used. A possible hypothesis that may explain these EID trends is that the methane concentration near the pilot spray has a more significant influence on the overall combustion rates than the pilot quantity itself over the range of Φ_{pilot} and $\Phi_{overall}$ investigated here.

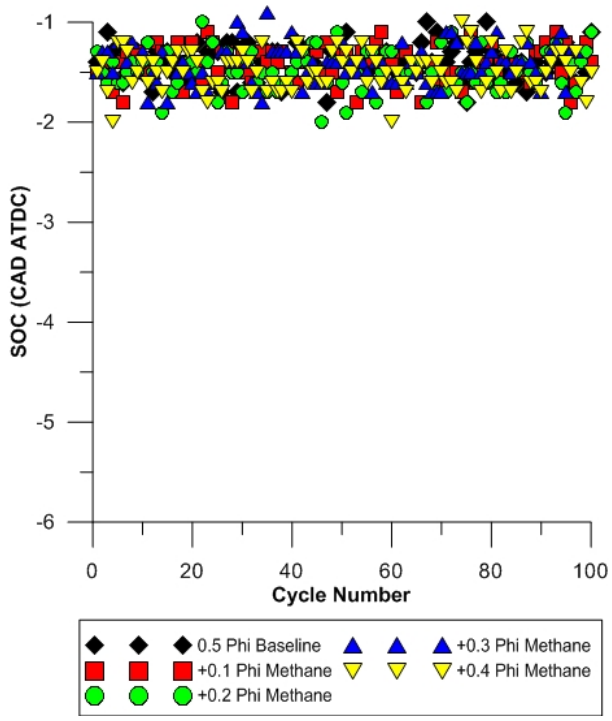

Figure 10. Cyclic variations in SOC for Φ_{pilot} = 0.5 and various methane concentrations ($\Phi_{overall}$ = 0.6, 0.7, 0.8, and 0.9) with a constant boost pressure of 1.4 bar and BMEPs ranging from 7.2 to 12.2 bar; standard deviations of SOC were 0.17, 0.17, 0.2, 0.19, and 0.19 CAD for $\Phi_{overall}$ of 0.5, 0.6, 0.7, 0.8, and 0.9, respectively.

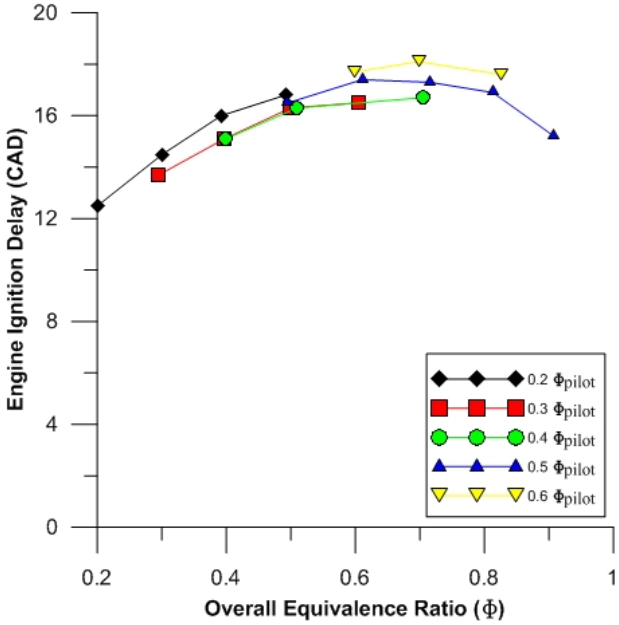

Figure 11. Engine ignition delay vs. overall equivalence ratio for diesel-ignited methane combustion; BMEPs ~ 1 bar to 12.9 bar; boost pressure maintained at baseline Φ_{pilot} value.

5.2.2 Percent Energy Substitution Effects on Ignition Delay

When methane is used as the primary fuel, its effect on ignition delay is quite pronounced as PES is increased at constant BMEP and also when BMEP is increased at constant PES (see Fig. 12). At lower BMEPs, the diesel quantity is very small; hence a small amount of methane is required to drastically increase the PES. Therefore, ignition delay is increased only slightly at lower BMEPs and PES, consistent with the trends observed in Fig. 9. However, at increased concentrations of methane at low BMEPs, the ignition delay tends to decrease as the engine operation becomes more unstable. At higher BMEPs, the amount of methane required to increase the PES also increases, and the ignition delay increase is also more significant. As noted in Ref. [12], oxygen displacement and chemical effects are contributors to this ignition delay trend, with the latter likely the more significant factor. In contrast to diesel-ignited propane combustion, the combination of these factors only tend to increase ignition delay when methane is used as the primary fuel, with the exception of high PES at low BMEPs.

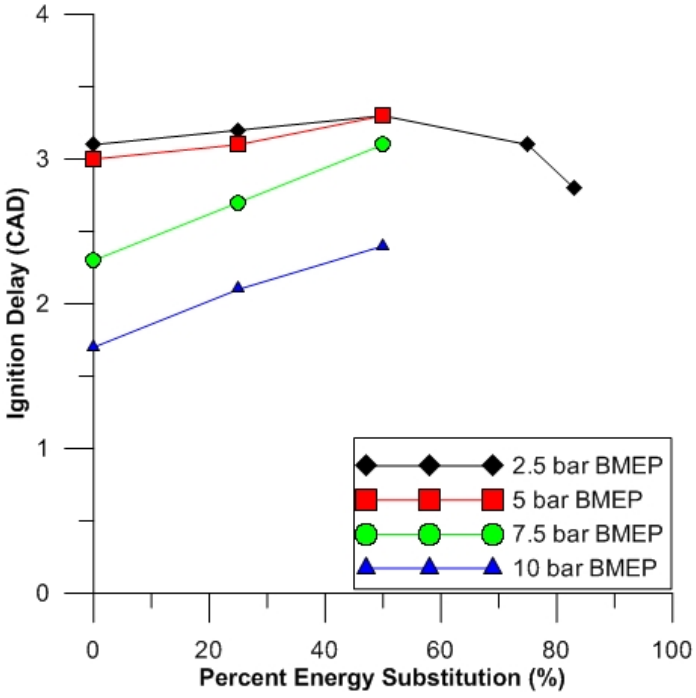

Figure 12. Ignition delay vs. PES at BMEPs of 2.5, 5, 7.5, and 10 bar for diesel-ignited methane combustion. Boost pressure was maintained at 0% PES value for a given BMEP (1.18bar, 1.28 bar, 1.40 bar, and 1.55 bar, respectively).

To gain additional insight regarding ID behavior at low BMEPs, the cyclic variations in SOC for diesel-ignited methane combustion at 2.5 bar BMEP is shown in Fig. 13. This condition is very similar to the 2.5 bar BMEP case shown in Fig. 8 for propane, with the exception that one additional set of data for 83 percent PES was able to be taken for methane. At this condition, the two primary fuels (propane and methane) seem to behave very similarly, with methane causing less of an increase in ID at lower PES. As with propane, the variation of SOC increases significantly with increasing PES, especially when engine operation becomes more unstable (COV of IMEP = 4.6) at 83 percent PES. Again, similar to propane, this instability is accompanied by a decrease in average ID.

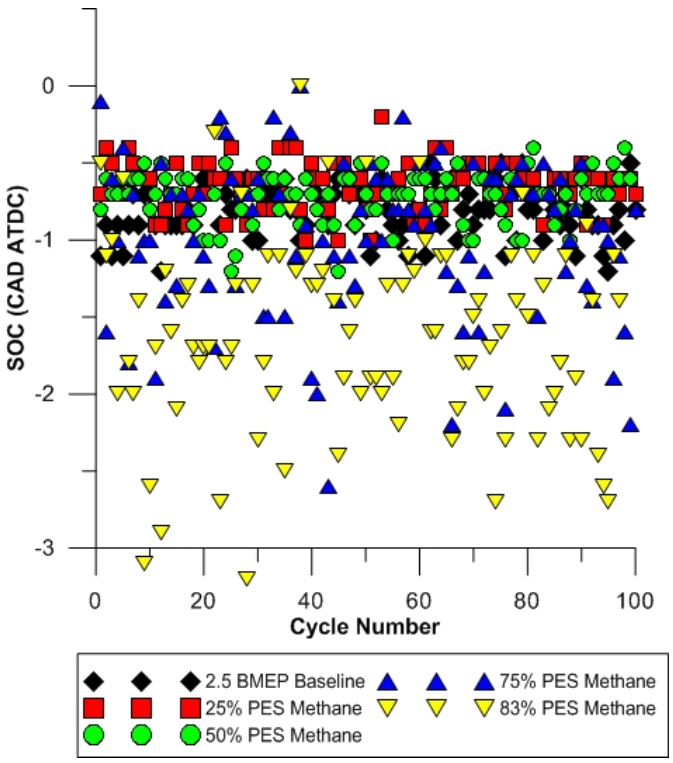

Figure 13. Cyclic variations in SOC for 2.5 bar BMEP and various PES of methane with constant boost pressure of 1.2 bar; standard deviations of SOC were 0.17, 0.16, 0.17, 0.51, and 0.63 CAD, respectively for 0, 25, 50, 75, and 83% PES.

6. CONCLUSIONS

Dual fuel ignition behavior was quantified experimentally for diesel-ignited propane and diesel-ignited methane combustion in a 1.9L VW TDI engine (with the stock ECU and a wastegated turbocharger) at a constant engine speed of 1800 rev/min. Two sets of experiments were performed. First, the effects of fuel-air equivalence ratios based on pilot fuel alone (Φ_{pilot}) and on both pilot and primary fuels ($\Phi_{overall}$) on ignition delay (ID) were investigated. Second, the effects of percent energy substitutions (PES) and BMEPs on ignition behavior were quantified. The following important conclusions can be drawn from the experimental results presented in this paper.

1. With constant but large Φ_{pilot} (>0.5), increasing propane concentration (to increase $\Phi_{overall}$) decreased ID. If $\Phi_{overall}$ was sufficiently high (>0.7), spontaneous autoignition (as

opposed to end-gas knock) of propane occurred before SOI of diesel pilot. Under similar conditions, increasing methane concentration had little effect on ID.

2. A cycle-by-cycle analysis of diesel-ignited propane combustion showed that for a constant Φ_{pilot}, cyclic variations in SOC increased as $\Phi_{overall}$ was increased. However, SOC variations decreased when in-cylinder conditions facilitated propane autoignition. A similar analysis of diesel-ignited methane combustion revealed very little cyclic SOC variations as $\Phi_{overall}$ was increased.
3. With increasing PES of propane at constant BMEP, different ID trends were obtained at low and high BMEPs. At low BMEPs, ID increased to a maximum and then decreased as engine instability increased. At high BMEPs, increasing PES of propane shortened IDs. By contrast for methane at low BMEPs, increasing PES only increased ID slightly. At higher BMEPs for methane, the increase in ID was more significant with increasing PES.
4. At low BMEPs, increasing PES led to a significant increase in cyclic SOC variations for both propane and methane. As cyclic SOC variations increased, the average SOC was advanced, thereby shortening the ID values for both diesel-ignited propane and diesel-ignited methane combustion.
5. The engine ignition delay (EID) was shown to be a useful metric to understand the influence of ID on dual fuel combustion. For propane at low Φ_{pilot}, the EID increased due to longer IDs and slower combustion rates. As Φ_{pilot} was increased, the higher reactivity of propane led to faster combustion rates and decreased EID significantly even with very small propane additions. For methane, the EID trends were nearly independent of pilot quantity. With increasing methane concentrations, the EID first increased, reached a maximum, and finally decreased. These trends imply that once ignition was achieved with diesel-ignited methane combustion, the ensuing combustion process was largely unaffected by the amount of pilot fuel used, at least for the conditions investigated in this work.

7. ACKNOWLEDGMENTS

The authors gratefully acknowledge financial support from the Sustainable Energy Research Center (US DOE Award # DE-FG36-06GO86025) and facilities support from the Center for Advanced Vehicular Systems at Mississippi State University. The views and opinions expressed herein are not necessarily those of the sponsoring agency or the university.

8. REFERENCES

1. **Karim, G. A.** (2003). Combustion in gas fueled compression-ignition engines of the dual fuel type. *Trans. ASME: Journal of Engineering for Gas Turbines and Power*, Vol. 125, pp. 827-836.
2. **Stewart, J., Clarke, A., and Chen, R.** (2007). An experimental study of the dual-fuel performance of a small compression ignition diesel engine operating with three gaseous fuels. *Proc. Inst. Mech. Engrs., Part D: Journal of Automobile Engineering*, Vol. 221, Issue 8, pp. 943-956.
3. **Srinivasan, K. K., Krishnan, S. R., Qi, Y., Midkiff, K. C. and Yang, H.** (2007). Analysis of diesel pilot-ignited natural gas low-temperature combustion with hot exhaust gas recirculation. *Combustion Science and Technology*, Vol. 179, Issue 9, pp. 1737-1776.
4. **Krishnan, S. R., Biruduganti, M., Mo, Y., Bell, S. R., and Midkiff, K. C.** (2002). Performance and heat release analysis of a pilot-ignited natural gas engine. *International Journal of Engine Research*, Vol. 3, Issue 3, pp. 171-184.
5. **A.S. Ramadhas, S. Jayaraj, C. Muraleedharan.** (2008). Dual fuel mode operation in diesel engines using renewable fuels: Rubber seed oil and coir-pith producer gas. *Renewable Energy*, Volume 33, Issue 9, pp. 2077-2083.
6. **Poonia, M. P., Ramesh, A., and Gaur, R. R.** (1999). Experimental investigation of the factors affecting the performance of a LPG – diesel dual fuel engine. SAE Paper 1999-01-1123.
7. **Papagiannakis, R. G. and Hountalas, D. T.** (2003). Experimental investigation concerning the effect of natural gas percentage on performance and emissions of a DI dual fuel diesel engine. *Applied Thermal Engineering*, Vol. 23, pp. 353–365.
8. **Karim, G. A.** (1987). The dual fuel engine. In *Automotive Engine Alternatives* (Ed. R. L. Evans), Plenum Press.
9. **Heywood, J. B.** (1988). *Internal Combustion Engine Fundamentals*, McGraw-Hill, Inc.
10. **Nielson, O. B., Qvale, B., and Sorenson, S.** (1987). Ignition delay in the dual fuel engine. SAE Paper 870589.
11. **Karim, G. A., Jones, W., and Raine, R. R.** (1989). An examination of the ignition delay period in dual fuel engines. SAE Paper 892140.
12. **Liu, Z. and Karim, G. A.** (1995). The ignition delay period in dual fuel engines. SAE Paper 950466.
13. **Gunea, C. Razavi, R. M., and Karim, G. A.** (1998). The effects of pilot fuel quality on dual fuel ignition delay. SAE Paper 982453.
14. **Prakash, G., and Ramesh, A.** (1999). An approach for estimation of ignition delay in a dual fuel engine. SAE Paper 1999-01-0232.
15. **Kalghatgi, G. T., Risberg, P., and Angstrom, H. K.** (2006). Advantages of fuels with high resistance to auto-ignition in late-injection, low-temperature, compression ignition combustion. SAE Paper 2006-01-3385.
16. **Gibson, C. M., Polk, A. C., Shoemaker, N. T., Srinivasan, K. K., and Krishnan, S. R.** (2011). Comparison of propane and methane performance and emissions in a turbocharged direct injection dual fuel engine. *Trans. ASME: Journal of Engineering for Gas Turbines and Power*, Vol. 133, Issue 9, Paper 092806, [DOI: 10.1115/1.4002895].

